BIOCHEMISTRY
including biophysical chemistry & molecular biology

Article

pubs.acs.org/biochemistry

Secondary Structure and the Role in Translation Initiation of the 5′-Terminal Region of p53 mRNA

Leszek Błaszczyk and Jerzy Ciesiołka*

Institute of Bioorganic Chemistry, Polish Academy of Sciences, Poznan 61-704, Poland

Supporting Information

ABSTRACT: The p53 protein is one of the major factors involved in cell cycle control, DNA repair, and induction of apoptosis. We determined the secondary structure of the 5′-terminal region of p53 mRNA that includes two major translation initiation codons AUG1 and AUG2, responsible for the synthesis of p53 and its N-truncated isoform ΔN-p53. It turned out that a part of the coding sequence was involved in the folding of the 5′ untranslated region for p53. The most characteristic structural elements in the 5′-terminal region of p53 mRNA were two hairpin motifs. In one of them, the initiation codon AUG1 was embedded while the other hairpin has been earlier shown to bind the Mdm2 protein. Alternative mechanisms of p53 mRNA translation initiation were investigated *in vitro* using model mRNA templates. The results confirmed that initiation from AUG1 was mostly cap-dependent. The process was stimulated by a cap structure and strongly inhibited by a stable hairpin at the template 5′ end. Upon inhibition, the remaining protein fraction was synthesized in a cap-independent process, which was strongly stimulated by the addition of a cap analogue. The translation initiation from AUG2 showed a largely cap-independent character. The 5′ cap structure actually decreased initiation from this site which argues against a leaky scanning mechanism but might suggest the presence of an IRES. Moreover, blocking cap-dependent translation from AUG1 by the stable hairpin did not change the level of initiation from AUG2. Upon addition of the cap analogue, translation from this site was even increased.

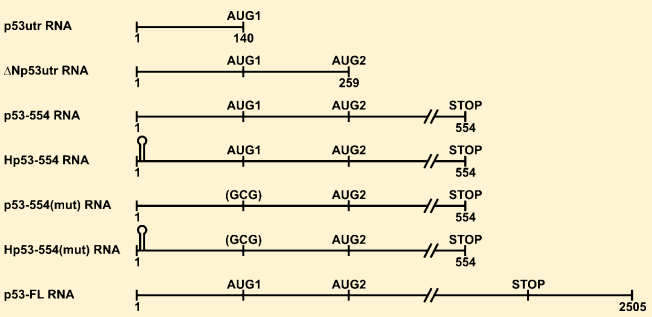

The p53 protein plays a key role in cell cycle control, DNA repair, and induction of apoptosis. The p53 gene is present in the human genome in a single copy comprising ca. 20 kb.[1−3] Eleven exons are present in the gene, of which the first exon and 28 nucleotides of the second one correspond to the 5′ untranslated region (5′ UTR) of p53 mRNA. The gene does not contain a typical transcription promoter, and a few transcription initiation sites are active.[1−3] It seems that promoter P1 is used most often and in that case the p53 5′ UTR totals ∼140 nucleotides. The ΔN-p53 isoform, which is also present in the cell, lacks the 39 N-terminal amino acids of full-length p53. The protein is synthesized as a result of translation initiation from the AUG codon localized in exon 4, and the length of 5′ untranslated region of mRNA increases to 257 nucleotides.[4,5] The ΔN-p53 isoform can bind to the full-length p53 protein, inhibiting its transcriptional activity and its activity as growth suppressor. Therefore, ΔN-p53 is thought act as a negative regulator of p53 during the course of the cell cycle.[4,6]

In normally functioning cells, the amount of p53 protein is low. The major regulator of the p53 level seems to be the Mdm2 protein.[1−3] The attachment of ubiquitin residues by Mdm2 is a signal to direct p53 to the proteasome, where it is degraded. It has recently been observed that the level of p53 mRNA remained unchanged although the level of p53 protein increased upon stress induction.[7] Therefore, it is postulated that increased efficiency of translation accompanies induction of p53 in the cell. The 5′ and 3′ untranslated regions of p53 mRNA and several proteins interacting with these regions may participate in the regulation of p53 expression at the translational level. It has been shown earlier that 5′ UTR plays an important role in the regulation of p53 synthesis. This region interacts with several proteins, which significantly affect the translation process. It is known that the full-length p53 has the ability to bind to the 5′ UTR of its own mRNA, inhibiting its translation,[8,9] although the nature of this interaction is still a matter of debate.[10] The next protein, which interacts with 5′ UTR, is ribosomal protein L26. It is assumed that L26 enables "getting around" the stable secondary structure of this region or it facilitates its unfolding, allowing induction of protein synthesis.[9] Very recently, it has been reported that in the binding of ribosomal protein L26 to human p53 mRNA and L26-dependent p53 induction base-pairing interactions between 5′ and 3′ UTR sequences are involved.[11] Another protein, nucleolin, may bind to the 5′ UTR, reducing translation of p53 and keeping a low level of p53 in a cell which has not been subjected to stressful conditions.[9] The polypyrimidine tract-binding protein (PTB) interacts specifically with both p53

Received: April 29, 2011
Revised: July 15, 2011
Published: July 19, 2011

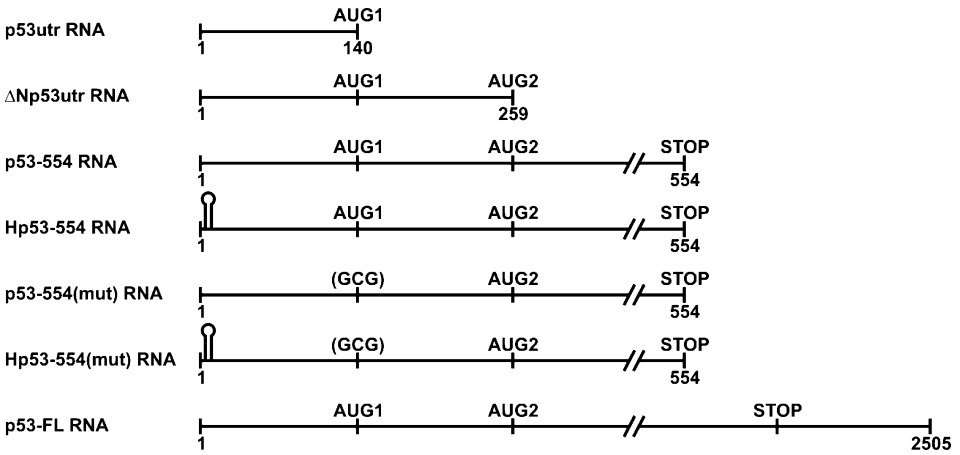

Figure 1. Schematic representation of the p53 mRNA constructs which were used in structural studies and *in vitro* translation assays. The 5′-terminal fragments of p53 mRNA are identical at their 5′ ends, and they begin with a sequence corresponding to the P1 transcription promoter of the p53 gene.[9,21] p53utr RNA corresponds to the 5′ UTR of p53 mRNA and includes the initiation AUG1 codon for the full-length p53 protein. In ΔN-p53utr RNA the 5′ UTR is extended by 120 additional nucleotides of the p53 coding sequence, and the fragment contains the AUG2 codon responsible for the initiation of the synthesis of the ΔNp53 isoform. p53-554 RNA comprises nucleotides 1 to 554 of the mature mRNA transcript and ends with the UGA stop codon. In three derivatives of p53-554 RNA, a thermodynamically stable hairpin is introduced at the 5′ end of Hp53-554 RNA, the initiation codon AUG1 is mutated to GCG triplet in p53-554(mut) RNA, and both these changes are present in Hp53-554(mut) RNA. Finally, p53-FL consists of 5′ UTR, ORF, and 3′ UTR. Nucleotide numbers 1−2505 in p53-FL correspond to 63−2567 in the p53 mRNA sequence (GenBank accession number NM_000546).

5′ untranslated regions, responsible for synthesis of the full-length and N-shortened protein isoforms. Silencing of PTB expression results in decreased translation of both p53 isoforms.[12] Interesting results have been published showing that Mdm2 binds to the extended 5′ UTR, presumably to its structural element of hairpin type, stimulating p53 translation.[13,14] The p53 5′ UTR seems to also be a target for the natural antisense transcript of p53, termed Wrap53, which regulates endogenous p53 mRNA levels and further induction of p53 protein.[15]

It has recently been shown that the 5′ UTR of p53 mRNA exerts properties of an IRES element, which enables internal initiation of translation.[7,16] Translation of the ΔN-p53 isoform also depends on the IRES element, which in this case includes the p53 5′ UTR extended by 117 additional nucleotides of the coding region. It has been suggested that these IRES elements determine the expression levels of the two p53 isoforms via their differential activities, thus playing an important role for cell cycle regulation.[16] The PTB protein, which has the ability to bind to the 5′ UTR of p53 mRNA, could function as a peculiar ITAF factor (IRES *trans*-acting factor) in this mechanism.[12]

In the aforementioned work concerning the functional role of the p53 5′ UTR in the regulation of protein expression, the importance of 5′ UTR folding has been postulated. Surprisingly, despite several studies on the functioning of p53 5′ UTR, there are no comprehensive experimental data published so far on the secondary structure of that mRNA region. The aim of our work was, therefore, to determine the secondary structure of the 5′-terminal region of p53 mRNA which includes two major translation initiation codons, responsible for the synthesis of the full-length protein and of its shorter isoform ΔN-p53. A recently proposed possibility of base pairing between the 5′ UTR and 3′ UTR was also addressed. In order to evaluate alternative mechanisms of p53 mRNA translation initiation selected mRNA constructs were used in *in vitro* translation studies.

EXPERIMENTAL PROCEDURES

DNA Template Constructs and RNA Synthesis. All oligodeoxyribonucleotides used in the construction of DNA templates were purified by electrophoresis on 12% polyacrylamide gels. DNA bands were excised, eluted with 0.3 M sodium acetate, pH 5.2, and 1 mM EDTA, and precipitated with 3 volumes of ethanol. DNA was recovered by centrifugation and dissolved in TE buffer. All DNA templates for variants of 5′ untranslated region of p53 mRNA described in this study (Figure 1) were amplified from human liver cDNA (Ambion) using the following forward and reverse primers: for ΔN-p53utr: FS, 5′-CTAGAGCCACCGTCCAGGGAGC-3′ and RL, 5′-TCCATTGCTTGGGACGGCAAGG-3′; for p53utr: FS and RS, 5′-TCCATGGCAGTGACCCGGAAGG-3′; for p53-554: FS and R295, 5′-GTCTTGGCCAGTTGG-CAAAACATC-3′; for p53-FL: FS and RUTR, 5′-TGGCAG-CAAAGTTTTATTGTAAAATAAGAGATCG-3′; for H56-169: FH, 5′-GTTCGGGCTGGGAGCGTG-3′ and RH, 5′-GCTCGACGCTAGGATCTGAC-3′. PCR reaction mixtures contained 0.5 ng of cDNA, 0.25 μM forward and reverse primers, 75 mM Tris-HCl, pH 8.8, 20 mM $(NH_4)_2SO_4$, 0.01% Tween 20, 1.5 mM $MgCl_2$, 200 μM each dNTP, and 1.25 units of Taq polymerase (MBI Fermentas). The reactions were performed on a Biometra T Gradient thermocycler for 30 cycles of initially 5 min at 95 °C, then 30 s at 95 °C, 30 s at 58 °C, 2 min at 72 °C, and finally 5 min at 72 °C. The reaction products were purified by phenol/chloroform (1:1, v/v) extraction and precipitated with ethanol. The obtained dsDNA templates were dissolved in TE buffer. p53utr dsDNA, ΔN-p53utr dsDNA, and p53-554 dsDNA were cloned into pRL-CMV vector (Promega). In the case of p53-FL dsDNA and H56-169 dsDNA, T7 promoter was added to the templates for subsequent RNA synthesis by *in vitro* transcription. The sequence of each construct was confirmed by sequencing.

Derivatives of the p53-554 construct were synthesized as follows. To prepare a Hp53-554 construct, we introduced a

dx.doi.org/10.1021/bi200659b | *Biochemistry* 2011, 50, 7080−7092

thermodynamically stable hairpin at the 5′ end of p53-554 construct using standard PCR technique (the hairpin sequence: 5′-GCGGTCCACCACGGCCGATATCACGGCCGTGGTG-GACCGC-3′). In the p53-554(mut) and Hp53-554(mut) constructs the AUG1 codon was mutated to GCG triplet using site-directed mutagenesis. The sequence of each construct was confirmed by sequencing.

The transcription reaction with AmpliScribe T7, T3, and SP6 High Yield Transcription Kit was performed as recommended by the manufacturer (Epicenter Biotechnologies). The RNA transcripts were purified on denaturing 8% polyacrylamide gels and labeled with ^{32}P at their 5′ or 3′ ends with polynucleotide kinase or T4 RNA ligase (MBI Fermentas) according to standard procedures. Capped RNA transcripts for *in vitro* translation experiments were synthesized using ARCA Cap Analogue (Epicenter Biotechnologies) as recommended by the manufacturer.

Pb^{2+}-Induced Cleavage. Prior to cleavage reaction with Pb^{2+} ions, the ^{32}P-end-labeled RNAs were renatured in the buffer: 40 mM NaCl, 10 mM Tris-HCl, pH 7.2, 10 mM $MgCl_2$ by heating for 5 min at 65 °C and slowly cooling to 37 °C. Electrophoresis of the renatured RNA molecules p53utr and ΔN-p53utr in nondenaturing polyacrylamide gels in the presence of 0.5, 2.5, and 10 mM Mg^{2+} ions showed major compact bands in each case, suggesting structural homogeneity of the RNA samples. The samples were then supplemented with tRNA carrier (Boehringer) to a final RNA concentration of 8 μM. Subsequently, lead acetate solution was added to the final concentration of 0.25, 0.5, or 1 mM, and the reactions proceeded at 37 °C for 5 min. The reactions were terminated by mixing their aliquots with 8 M urea/dyes/20 mM EDTA solution. Then the samples were loaded on 12% polyacrylamide, 0.75% bis-acrylamide, and 7 M urea gels. Electrophoresis was performed at 2000 V for 2−3 h, followed by autoradiography at −70 °C with an intensifying screen or phosphorimaging with Typhoon 8600 analyzer (Molecular Dynamics) or Fluor Imager FLA-5100 (FujiFilm).

In order to assign the cleavage sites, products of metal-ion induced cleavage of 5′- or 3′-end-^{32}P-labeled RNA were run along with the products of alkaline RNA hydrolysis and limited T1 nuclease digestion of the same RNA. An alkaline hydrolysis ladder was generated by incubation of the RNA with 5 volumes of formamide at 100 °C for 10 min. Partial T1 nuclease digestion was performed in 50 mM sodium citrate, pH 5.3, 7 M urea with 0.2 U of the enzyme at 55 °C for 10 min. In some experiments unlabeled RNAs were used in Pb^{2+}-induced cleavage reactions. In order to determine the cleavage sites, the primer extension method was used in that case.

SHAPE Analysis. The reaction mixture containing 20 pmol of RNA (0.4 μM final concentration) in renaturation buffer (10 mM Tris pH 8.0, 100 mM KCl, and 0.1 mM EDTA), and in final volume of 20 μL, was heated at 90 °C for 3 min and slowly cooled (0.1 °C/s) to 4 °C. The folding buffer (40 mM Tris pH 8.0, 5 mM $MgCl_2$, 130 mM KCl, and 0.1 mM EDTA) was then added and water to final volume of 146 μL. The sample was incubated at 37 °C for 10 min and separated into two reactions. The RNA solution was mixed with 3.4−7.3 μL of 180 mM *N*-methylisatoic anhydride (NMIA; Invitrogen) in DMSO (8−16 mM final concentration). The control reaction contained DMSO without NMIA. Both reactions were incubated for 50 min at 37 °C (50 or 60 °C in temperature melting experiments), and RNA was precipitated with 0.3 M sodium acetate, pH 5.2, 1 μL of glycogen (20 mg/mL), and 3 volumes of ethanol. After centrifugation RNA was resuspended in 10 mM Tris pH 8.0 and 0.1 mM EDTA.

Primer Extension. The primer extension reaction was performed by mixing modified RNA (2 pmol), 5′-end-^{32}P-labeled DNA primer (2 pmol) and water in final volume of 12 μL. The reaction mixture was incubated at 95 °C for 1 min, at 60 °C for 5 min and at 52 °C for 2 min, and then 8 μL of reverse transcription mix was added; final reaction conditions: 50 mM Tris-HCl pH 8.3, 75 mM KCl, 3 mM $MgCl_2$, 6 mM DTT, 500 μM each dNTP, and 50 units of reverse transcriptase (Superscript III, Invitrogen). The reactions were performed at 52 °C for 10 min. cDNA samples were then treated with 1 μL of 4 M NaOH, placed on ice, heated at 95 °C for 5 min, placed on ice, and treated with 160 mM Trizma. Dideoxy sequencing markers were generated in the same way using unmodified RNA and thymidine or adenosine dideoxy terminating nucleotides (0.2 mM). In the next step cDNAs were precipitated with 0.3 M sodium acetate, pH 5.2, 1 μL of glycogen (20 mg/mL), and 3 volumes of ethanol. After centrifugation cDNAs were resuspended in water. Following addition of 8 M urea/dyes/20 mM EDTA solution the samples were denatured for 2 min at 95 °C and loaded on 8% polyacrylamide, 0.75% bis-acrylamide, 7 M urea gels. Electrophoresis was performed at 2000 V for 2−3 h, followed by phosphorimaging with Typhoon 8600 analyzer (Molecular Dynamics).

Computer Analysis of SHAPE Data and RNA Structure Prediction. Bands that corresponded to NMIA modified nucleotides and those present in the control lane were integrated using Semi-Automated Footprinting Analysis (SAFA) software to obtain numerical output of the band intensities.[17] Raw intensities were normalized using the noRNAlize program.[18] The program works under Matlab environment and performs statistical analyses of the weak signals from NMIA modifications, subsequently using that information for signal normalization. All secondary structure predictions were performed by using the RNAstructure 4.6 program.[19,20] Normalized SHAPE intensities were entered as pseudo-free energy constraints to obtain secondary structures for all studied RNA molecules.

Nuclease Mapping. Prior to nuclease mapping, the ^{32}P-end-labeled RNA was supplemented with unlabeled RNA (10 pmol in total reaction volume of 20 μL) and was subsequently renatured in the buffer: 40 mM NaCl, 10 mM Tris-HCl, pH 7.2, 10 mM $MgCl_2$ by heating for 5 min at 65 °C, and slowly cooling to 37 °C. The digestion reactions were performed with different amounts of ribonuclease A or T1 at 37 °C. The reactions were terminated by adding equal volumes of 8 M urea/dyes/20 mM EDTA solution and immediate freezing the samples on dry ice. The reaction products were analyzed by polyacrylamide gel electrophoresis and visualized by phosphorimaging. In some nuclease mapping experiments only unlabeled RNA was used, and the cleavage sites were determined by the primer extension method.

***In Vitro* Translation.** *In vitro* translation experiments were carried out in the rabbit reticulocyte lysate system, nuclease treated (RRL; Promega) as recommended by the manufacturer. Briefly, the reaction mixture containing 17.5 μL of RRL, 20 μM

amino acid mixture minus methionine, 1 μL of [^{35}S]methionine (1000 Ci/mmol) (Hartmann Analytic), 20 units of RNasin ribonuclease inhibitor (Promega), and 5 pmol of capped or uncapped RNA in the final volume of 25 μL was incubated for 90 min at 30 °C. For experiments with the cap analogue (m^{7}GpppG) as an inhibitor rabbit reticulocyte lysate was preincubated for 15 min at 30 °C with increasing concentration of the cap analogue (0−1000 μM) and equimolar amounts of magnesium acetate. Translation products were resolved on SDS−polyacrylamide gels followed by radioisotope imaging with FLA 5100 image analyzer (Fuji). Band intensities were analyzed using MultiGauge software (Fuji).

RESULTS

A Fragment of p53 Coding Sequence Is Involved in Folding of the 5′ UTR. The p53 mRNA fragment ΔN-p53utr RNA includes two initiation codons: AUG1 for synthesis of the full-length p53 and AUG2 for translation of the N-truncated p53 isoform (Figure 1). The Pb^{2+}-induced cleavage and SHAPE (selective 2′-hydroxyl acylation analyzed by primer extension) probing data for this RNA are shown in Figure 2 (the autoradiograms of SHAPE analysis are presented in Figure S1). The Pb^{2+}-induced cleavage method has been earlier shown to monitor flexibility of RNA polynucleotide

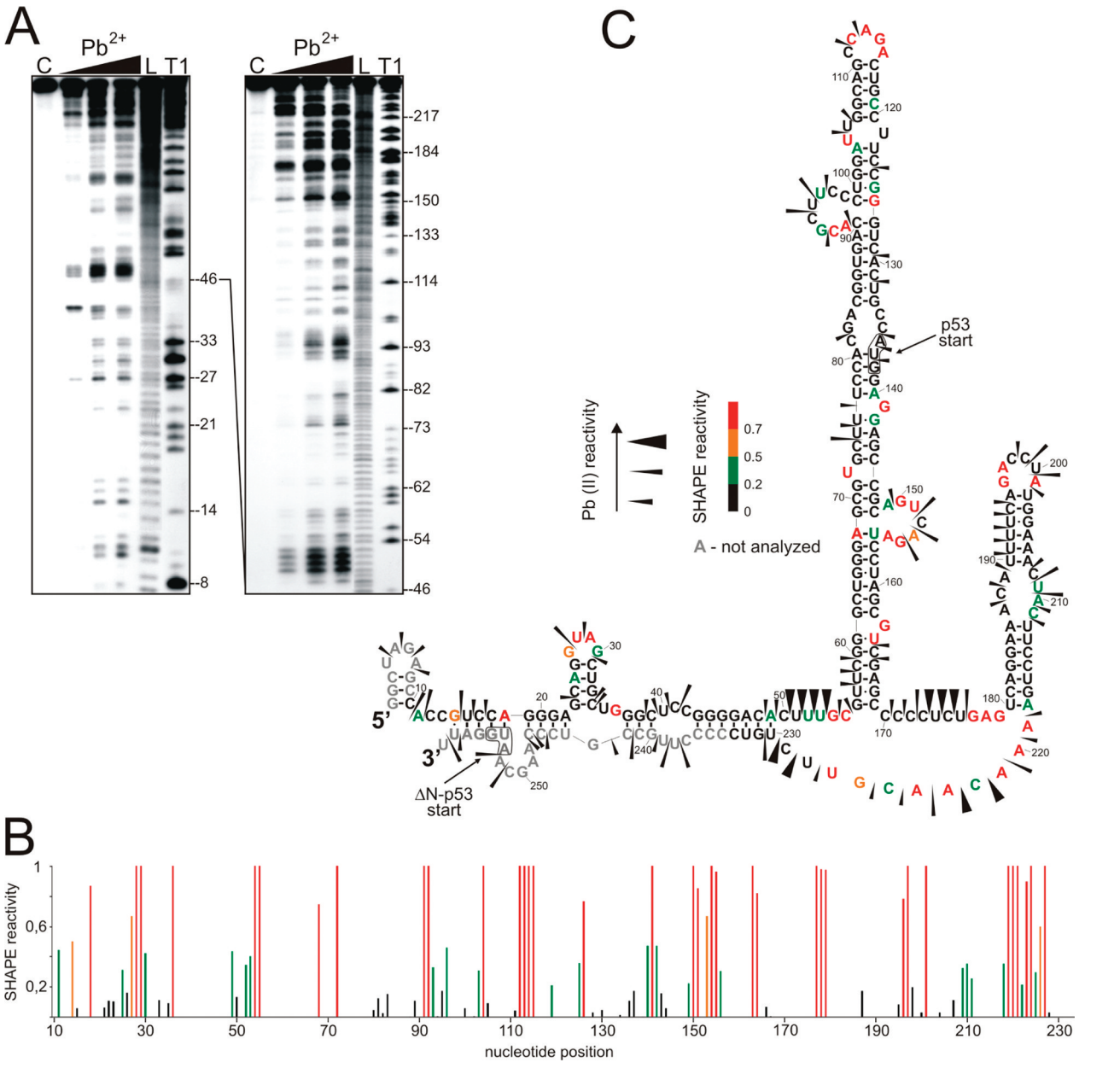

Figure 2. Structural probing of ΔN-p53utr RNA by Pb^{2+}-induced cleavage and SHAPE methods. (A) Autoradiograms show the products of Pb^{2+}-induced cleavage reactions analyzed on 12% polyacrylamide gels in denaturing conditions. The reactions were carried out with 5′-^{32}P-end-labeled RNA at 37 °C with 0.25, 0.5, and 1 mM Pb^{2+} ions for 5 min. Lanes: C, control reaction; L, formamide ladder; T1, limited hydrolysis by RNase T1 in denaturing conditions. Selected guanine residues are labeled on the right. (B) Normalized SHAPE reactivities as a function of nucleotide position. Bars are colored using the scheme shown in panel C. (C) Secondary structure model of ΔN-p53utr RNA. Relative intensities of Pb^{2+} cleavages correlate with the size of black triangles. Nucleotide symbols are colored (black, green, orange, red) according to their SHAPE reactivities. Nucleotides which were not analyzed are in gray.

dx.doi.org/10.1021/bi200659b | Biochemistry 2011, 50, 7080−7092

chains.[22−27] Single-stranded or distorted helical regions are cleaved in the presence of Pb^{2+} ions while rigid double-stranded stretches are resistant to cleavage. In principle, the method lacks base specificity although relatively weak cleavages are usually observed to occur at guanosine residues. The method is very informative in detecting not only substantial differences in Watson−Crick base pairing but also subtle differences in the RNA conformation resulting from changes in stacking or tertiary interactions.[22−27] Similar structural specificity as in the case of the Pb^{2+}-induced cleavage method is claimed to be characteristic for the SHAPE approach that has recently been introduced to RNA structural studies.[28] In this approach *N*-methylisatoic anhydride (NMIA) is used which preferentially modifies ribose 2′ hydroxyl groups localized in flexible regions of RNA polynucleotide chains. Some constrained ribose residues of atypical 2′-endo conformation seem to also undergo modification.[18] More recently, the influence of base identity on the intrinsic reactivity of each nucleotide toward NMIA has been precisely analyzed.[29] It turns out that G and A residues have identical 2′-hydroxyl reactivity but are 1.4 and 1.7 times more reactive than U and C, respectively. However, these subtle differences are much smaller than those observed for paired and unpaired nucleotides and thus do not impact the ability of the SHAPE method to monitor RNA folding.[29]

The secondary structure presented in Figure 2 is the most stable arrangement of ΔN-p53utr RNA (ΔG = −116 kcal/mol) predicted *in silico* by the RNAstructure 4.6 program, in which the results of SHAPE probing have been included. The structure is also consistent with the results of the Pb^{2+}-induced cleavage method and the known specificity of that approach.[22−24] The most characteristic structural features of the proposed fold include a long hairpin domain spanning nucleotides G56-C169 in which the AUG1 codon is embedded, another shorter hairpin formed by the region U180-A218, and a region of secondary interactions between the 5′-proximal stretch G14-A49 and a fragment of the coding sequence, U258-U230, which includes the AUG2 codon. Structural distortions present within the long G56-C169 hairpin domain are well mapped with the NMIA reagent. In particular, this concerns modification of nucleotides in two large asymmetric bulges: A91-C98 and A149-A155, nucleotides within the apical loop (C111-A115), and single-nucleotide bulges: U72, G141, and G163. The loop regions are also recognized by Pb^{2+} ions although cleavages are less uniformly distributed in these stretches. This seems to be a consequence of the lower reactivity at purine (particularly G) residues.[22−24] As regards the second hairpin U180-A218, the NMIA and Pb^{2+} probes recognized its apical loop; however, no Pb^{2+}-induced cleavage was observed at the two 5′-proximal purines of the loop. Pb^{2+} ions mapped the asymmetric internal bulge in hairpin U180-A218 as well as the polypyrimidine stretch U190-C194 on the 5′-side of the terminal stem region predicted to be relatively unstable. The presence of two characteristic hairpins G56-C169 and U180-A218 in the ΔN-p53utr RNA was also consistent with our results of T1 digestion and DMS modification studies. Strong RNase T1 cleavages occurred in single-stranded bulge regions at G93, G114, G150, G154, and G196 (Figure S6) while DMS modified residues, predominantly C and A, in the apical loop of both hairpins and within the internal loop of hairpin U180-A218 (data not shown).

The proposed secondary interactions between the 5′- and 3′-terminal regions of ΔN-p53utr RNA are supported by experimental probing data. The formation of a short hairpin G23-C34 is consistent with both the NMIA and Pb^{2+} probing results. Pb^{2+} ions also cleave regions C39-C41 and C237-U239 within a symmetric internal loop. However, this loop is not recognized by NMIA. This concerns the upper strand of the secondary structure shown in Figure 2C while the bottom strand escaped analysis as being involved in hybridization to an oligonucleotide primer used in reverse transcription. The SHAPE approach seems to be less diagnostic than the Pb^{2+} method in recognizing the internal loop present in the U180-A218 hairpin. Moreover, Pb^{2+} ions allow better identification of some double-stranded RNA regions of presumably low stability. For example, such regions are detected between U190 and A195 and between G56 and C59. Lower ability of the SHAPE approach to map some internal bulges and thermodynamically unstable double-stranded regions may result, at least partly, from losing some signals of low intensity during data processing. Usually higher background, which is visible on gel autoradiograms with reverse transcription products of the SHAPE analysis in comparison with Pb^{2+}-induced cleavage products of ^{32}P-end-labeled RNA, requires a more stringent cutoff procedure. Finally, the single-stranded stretches C50-C55, C170-G179, and A219-C229 are well mapped both by the Pb^{2+} cleavage method and the SHAPE approach. A striking exception is the C170-U176 region, which is unreactive in the SHAPE analysis.

The results of structural probing of p53utr RNA are shown in Figure 3 and Figure S1. It turns out that the RNAstructure 4.6 program with SHAPE constraints proposes for this RNA a few secondary structures with very similar stabilization energies. In Figure 3C, the structure with stabilization energy of −59.8 kcal/mol is shown. In the alternative computer proposition with stabilization energy of −61.8 kcal/mol, a new helix composed of 5 bp is formed by interaction of the U15-G19 and A103-C99 regions, whereas the sequence stretches G20-U64 and U121-A140 are folded in two and one hairpin motif, respectively (in the figure, these two sequence stretches are marked and their alternative arrangements are shown). In the alternative structure three hairpin motifs are preserved: G1-C10, G65-C98, and G106-C120. Both the computer predicted secondary structures of p53utr RNA are essentially consistent with the results of Pb^{2+} probing and SHAPE analysis. One may speculate that this RNA fragment folds into a mixture of conformational forms. However, gel electrophoresis of the RNA sample in nondenaturing conditions revealed one major band contradicting this assumption (data not shown). In any case, the most important observation of structural probing of p53utr RNA is that the fragment folds in a different manner than the corresponding sequence of ΔN-p53utr RNA. The only element that is common to both secondary structures is hairpin motif G106-C120.

Secondary Structure of the ΔN-p53utr RNA Is Preserved within Longer mRNA Fragments and in the Full-Length p53 mRNA. In order to find out whether other downstream mRNA regions may affect folding of the two characteristic hairpin elements (G56-C169 and U180-A218) in ΔN-p53utr RNA, we synthesized p53-554 RNA (Figure 1). The fragment comprised 554 nucleotides from the 5′-terminus of p53 mRNA and included approximately half of its coding sequence. The secondary structure of p53-554 RNA was

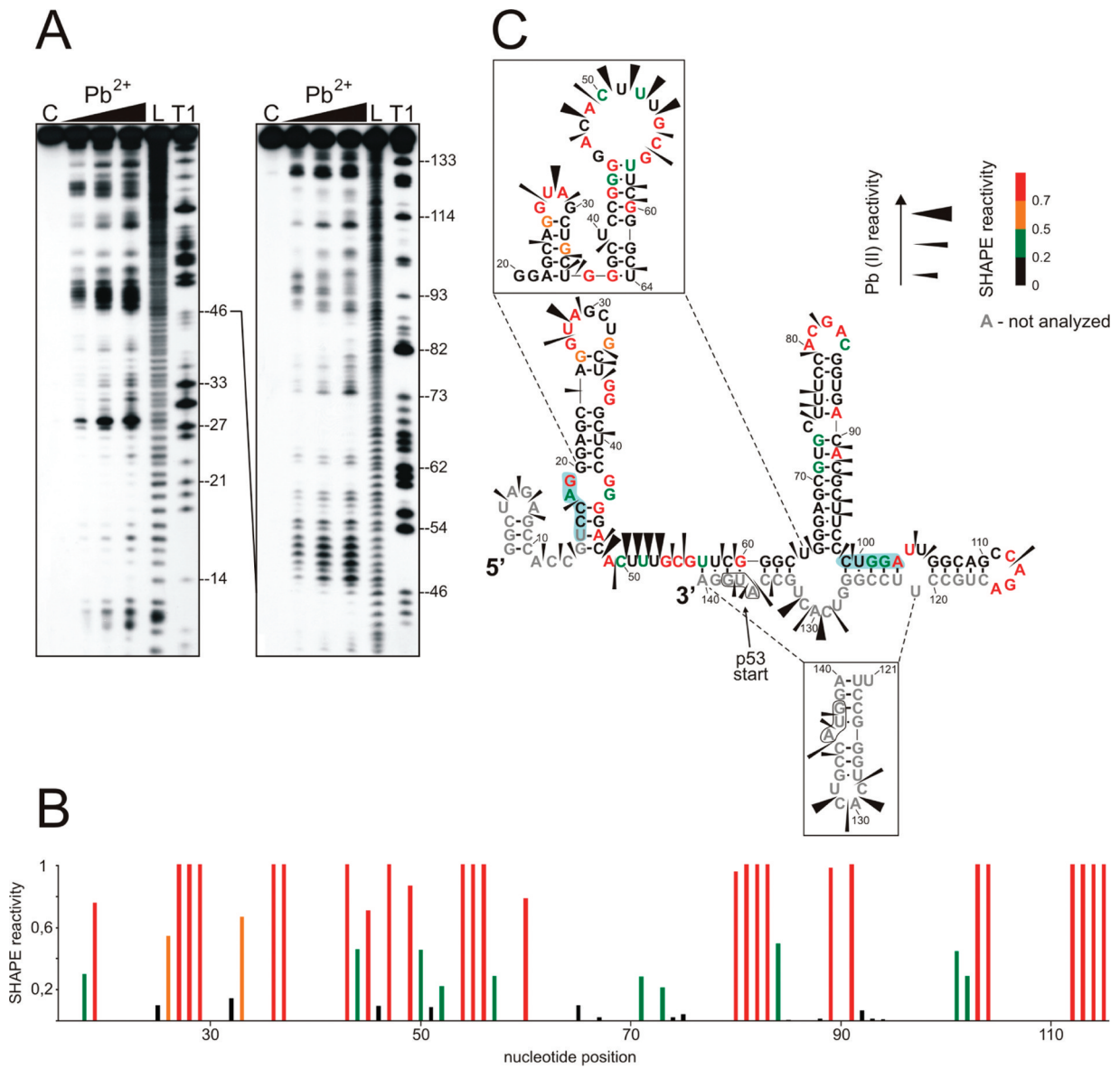

Figure 3. Probing of the structure of p53utr RNA. (A) Autoradiograms of Pb^{2+}-induced cleavage products of the p53utr RNA. The reactions were carried out with 5′-^{32}P-end-labeled RNA. Lanes: C, control reaction; L, formamide ladder; T1, limited hydrolysis by RNase T1 in denaturing conditions. Guanine residues are labeled on the right. (B) Normalized SHAPE reactivities as a function of nucleotide position. (C) Cleavages induced by Pb^{2+} ions are displayed on the secondary structure model of p53utr RNA that is most consistent with experimental data. Alternative arrangements of two regions: G20-U64 and U121-A140 are also shown in the insets (details in the text). Nucleotide symbols are colored to reflect their SHAPE reactivities.

analyzed using the Pb^{2+}-induced cleavage method and the SHAPE approach (Figures 4 and 5 and Figure S2). The data for the region which spans nucleotides G43 and C236 are summarized in Figure 4C. A comparison of the obtained patterns with those characteristic of the corresponding region of ΔN-p53utr RNA (Figure 2C) clearly shows that both RNA sequences are folded very similarly. Minor differences concern the lack of Pb^{2+} cleavages in the C74-U76 region in p53-554 RNA, stronger cleavages in the A91-C98 and A155-U159 regions, and a few additional cleavages or changes in cleavage intensity at single nucleotide positions in other regions. The SHAPE approach revealed differences predominantly at the bottom of the G56-C169 hairpin, namely at C50-C55 and U228-G231, which showed increased reactivity in the p53-554 RNA (Figure 4C). We also observed slightly stronger modification of some nucleotides close to the initiation codon as well as in the upstream U128-A130 stretch. Despite these minor differences, the experimental data support the presence of both hairpin motifs G56-C169 and U180-A218 in the p53-554 RNA.

The presence of the large hairpin domain, which spans nucleotides G56 and C169, seems to be particularly important for folding of the 5′-terminal sequence of p53 mRNA. This domain is relatively stable (ΔG = −52.9 kcal/mol), and in its central part the AUG1 codon is located. H56-169 RNA, an oligoribonucleotide with the sequence identical to the hairpin motif, was synthesized, and its secondary structure was analyzed with the Pb^{2+}-induced cleavage and SHAPE methods (Figure S7). It turns out that the pattern of Pb^{2+} cleavages is very similar to that characteristic of the corresponding region in

dx.doi.org/10.1021/bi200659b | *Biochemistry* 2011, 50, 7080–7092

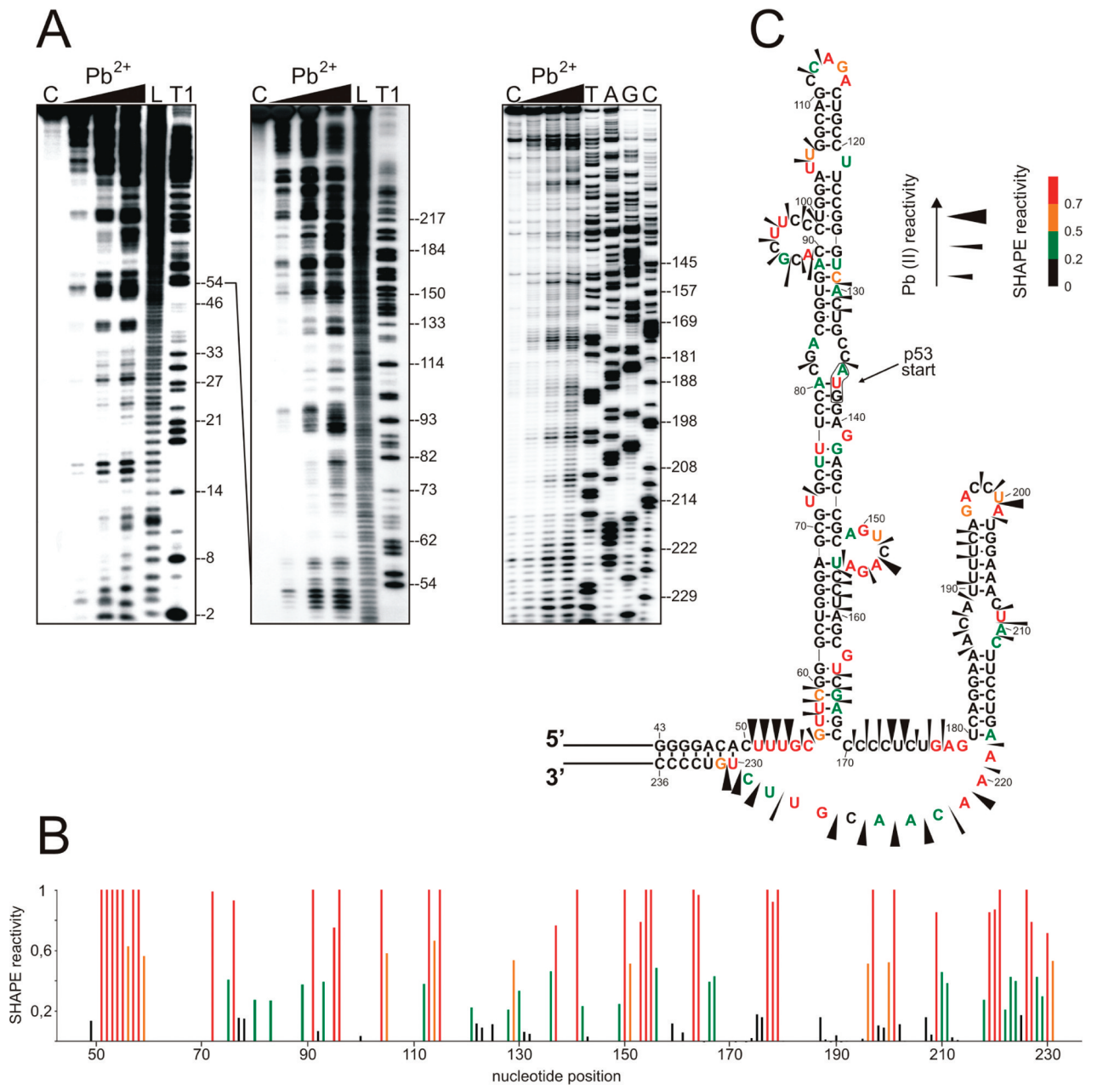

Figure 4. Secondary structure arrangement of the sequence stretch between G43 and C236 in the p53-554 RNA. (A) Autoradiograms show the products of Pb^{2+}-induced cleavage of 5′-^{32}P-end-labeled RNA (left two panels) and the products of primer extension analysis (right panel). Lanes: C, control reaction; L, formamide ladder; T1, limited hydrolysis by RNase T1 in denaturing conditions; T,A,G,C denote lanes with sequencing reactions performed in the presence of thymidine, guanosine, adenosine, and cytosine dideoxy terminating nucleotides. Selected guanine and cytosine residues are labeled on the right. (B) Normalized SHAPE reactivities are shown as colored bars. (C) A part of the secondary structure model of p53-554 RNA (nucleotides 43-236). Cleavages induced by Pb^{2+} ions as well as SHAPE data are displayed in the figure.

p53-554 RNA (Figure 4C). Minor differences concern higher accessibility to cleavage of two asymmetric bulges A91-C98 and A149-A155 in the H56-169 RNA. Thus, on the basis of results of such "structural fingerprinting", we can conclude that the G56-C169 region folds into the proposed hairpin motif also in p53 mRNA. This conclusion is also consistent with the results of SHAPE analysis of H56-169 and ΔN-p53utr RNAs (Figure 2 and Figure S7), although in the shorter fragment, some additional nucleotides were modified within the internal loop close to AUG initiation codon (discussed later in the text).

In order to find out whether the two characteristic hairpins G56-C169 and U180-A218 are formed in the full-length p53 mRNA context, p53-FL RNA (5′ UTR, ORF and 3′ UTR; Figure 1) was analyzed. This RNA was subjected to Pb^{2+} cleavage and SHAPE probing (Figures S3 and S5). It turns out that the secondary structure of 5′-terminal region of p53-FL is highly similar to that determined for ΔN-p53utr and p53-554 RNAs. This further supports our observation that p53 5′ UTR assumes a highly organized and stable secondary structure. Finally, a model mRNA construct in which the ΔN-p53utr was followed by a sequence encoding the reporter protein luciferase was synthetized. Structural mapping of this construct by the Pb^{2+} cleavage, SHAPE, and DMS modification methods confirmed the presence

dx.doi.org/10.1021/bi200659b | Biochemistry 2011, 50, 7080–7092

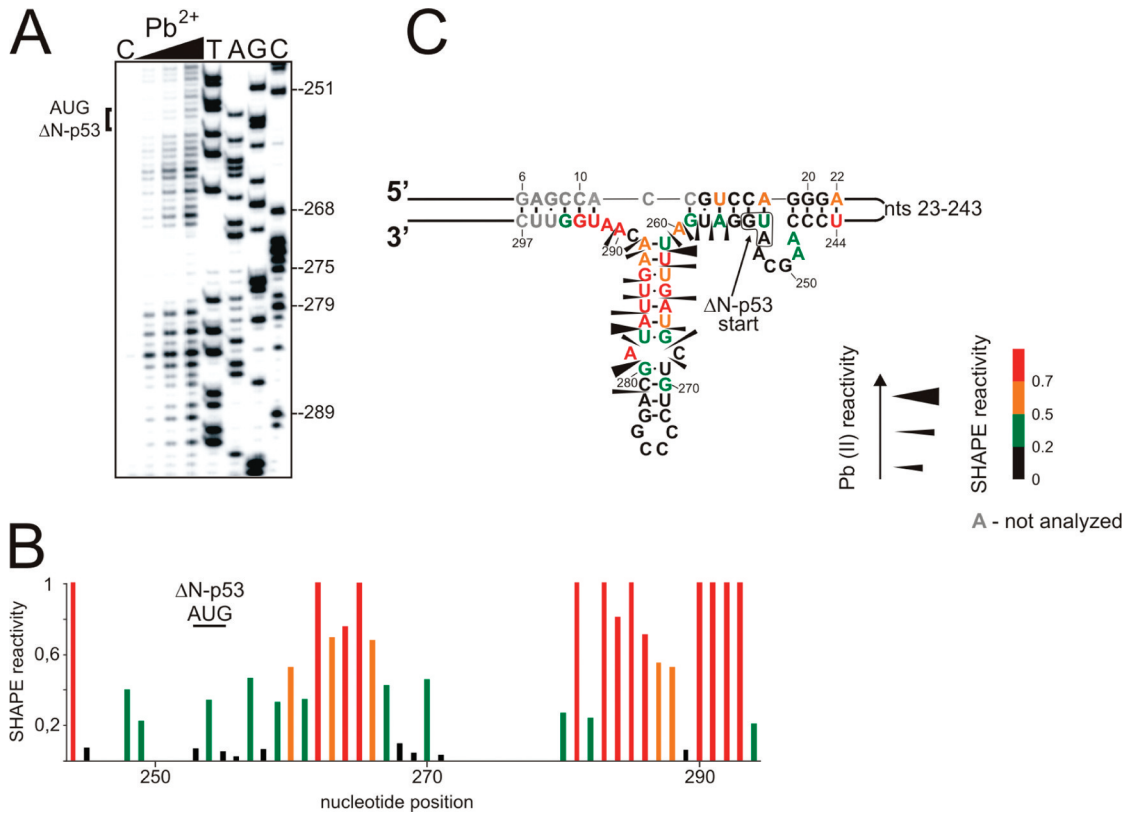

Figure 5. Structural environment of the initiation codon for the ΔN-p53 isoform within p53-554 RNA. (A) Autoradiogram shows the products of Pb^{2+}-induced cleavage reaction analyzed by primer extension. Lanes: C, control reaction; T, A, G, C, sequencing reactions with thymidine, adenosine, guanosine, and cytosine dideoxy terminating nucleotides. Selected cytosine residues are labeled on the right. (B) Normalized SHAPE reactivities as a function of nucleotide position. Bars are colored using the scheme shown in panel C. AUG codon for ΔN-p53 protein is marked. (C) Structural environment of ΔN-p53 initiation codon. Relative intensities of Pb^{2+} cleavages correlate with the size of black triangles. Nucleotides are colored (black, green, orange, red) according to their SHAPE reactivities.

of characteristic hairpin G56-C169 in which the AUG1 initiation codon is located. Moreover, DMS probing in rabbit reticulocyte lysate (RRL) showed that this hairpin is also preserved in conditions in which translation assays were performed (Górska et al., unpublished results of our laboratory). Since it seems that translation of p53 in RRL resembles its translation *in vivo*,[9,16] the structural environment of AUG1, as determined in our study, likely reflects the structure of this region in native conditions.

Recently, Chen and Kastan[11] have provided experimental data demonstrating that binding of ribosomal protein L26 and p53 translational stimulation are enhanced by the additional presence of the 3′ UTR of p53 mRNA. On the basis of nuclease digestion data and the analysis of mutation effects, they have proposed the existence of a double-stranded RNA region containing complementary sequences of the 5′ and 3′ UTRs. The region of 5′ UTR presumably involved in such interactions would involve in our model the stretch between G82 and G102 (Figure 4). However, the patterns of Pb^{2+} cleavage (Figure S5) and SHAPE modification (Figure S3) of this region in FL-p53 were essentially identical to those observed for ΔN-p53utr (Figure 2 and Figure S1) and p53-554 RNAs (Figure 4 and Figures S3 and S4). Moreover, the RNase A and T1 mapping data, which were obtained for FL-p53 and ΔN-p53utr RNAs, supported our secondary structure model of the 5′-terminal region of p53 mRNA and showed that it is not changed in the full-length molecule (Figure S6). It is not clear why we were unable to detect the 5′−3′ UTR interactions proposed by Chen and Kastan.[11] One may suggest that the explanation of their functional data may require taking into account the possibility of more complex structural interactions that in addition to 5′ and 3′ UTRs involve protein cofactors L26, Mdm2, and PTB interacting with these regions.

Structural Context of the Initiation Codons Might Influence Translation Initiation. Figure 4C shows the structural environment of the initiation codon for the full-length p53 protein and Figure 5C for its N-truncated isoform, as it was determined in our study. Interestingly, in both cases the AUG triplets are localized at single-strand/helix junctions. The A residues are unpaired in either symmetric 3/3 internal or asymmetric 6-nucleotide-membered loops.

The ability of structurally constrained AUG codons to initiate translation will require changes of their environment to occur. Such changes may take place due to thermodynamic instability of the neighboring structural elements or they may be induced by protein or other factors that bind in the vicinity. In binding of such effectors two large bulges may be potentially engaged that are present above and below the AUG1 codon in the secondary structure of the G56-C169 hairpin motif (Figure 4C). In the vicinity of the AUG2 codon there is a thermodynamically unstable hairpin U261-A288 (Figure 5C), which is composed mostly of AU and GU base pairs (ΔG = −4.4 kcal/mol). The hairpin may take part in the

dx.doi.org/10.1021/bi200659b | *Biochemistry* 2011, 50, 7080−7092

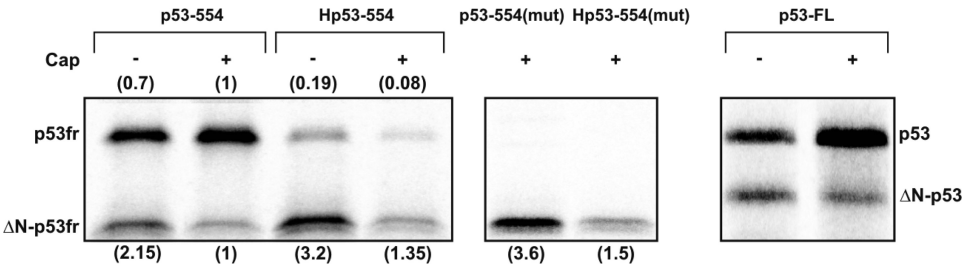

Figure 6. *In vitro* translation of p53 and ΔN-p53 proteins and their C-truncated fragments, p53fr and ΔN-p53fr, in rabbit reticulocyte lysate (RRL). *In vitro* transcribed model p53 mRNA templates, which are schematically depicted in Figure 1, were translated in RRL in the presence of ^{35}S-methionine and the relative amounts of translation products: p53, ΔN-p53, p53fr, and ΔN-p53fr were determined. The quantitative data were calculated based on at least three independent experiments.

translational regulation of the shorter protein isoform, for example, by binding of specific protein factors.

To gain more information on thermodynamic stability of structural elements surrounding the AUG1 codon, we followed temperature melting of ΔN-p53utr RNA by means of the SHAPE approach (Figure S8). Although the overall secondary structure of this RNA is preserved in the temperature range of 37 and 60 °C, some nucleotides have changed their reactivity. In particular, the nucleotide stretch A136-G142, which includes the AUG1 codon, as well as G82 and A83 on the 5′-side of the internal loop became more reactive at higher temperature. Thus, the structural environment of the initiation codon seems to be thermodynamically less stable than other elements of the G56-C169 hairpin. Another region that has changed its reactivity is a part of the polypyrimidine tract between C172 and U176. This region is not modified by NMIA at 37 °C due to unknown reasons, although it is very strongly cleaved by Pb^{2+} ions (Figure 2). However, it is mapped as a single-stranded RNA stretch by NMIA at 60 °C. Also the polypyrimidine track C50-U53 located nearby in the secondary structure model undergoes stronger modification upon temperature rising. It has been shown that the PTB protein interacts specifically with the p53 5′ UTR and the 5′ UTR extended by the sequence encoding the first 39 amino acids and that the binding site seems to be located downstream of the first AUG codon.[12] Possibly, the polypyrimidine stretch C172-U176 that changes its reactivity toward NMIA upon temperature rising might be involved in this interaction. Finally, the sequence G203-A207 becomes modified by NMIA at a higher temperature. That sequence is a part of a characteristic hairpin, which has been earlier shown to bind to the Mdm2 protein.[13,14] Summarizing, our temperature melting data for ΔN-p53utr RNA reveled three major regions of relatively low thermodynamic stability. One of these regions includes the initiation codon while the other two regions have been earlier proposed to interact with PTB[12] and Mdm2,[13,14] which seem to be involved in the regulation of p53 expression at the translational level.

Relative Amounts of p53 and ΔNp53 Translation Products Depend on the Presence of Cap and Stable Hairpin Structures at the 5′ End of Model mRNA Templates. We set out to investigate alternative mechanisms of p53 mRNA translation initiation that control the expression of the full-length p53 protein and ΔNp53 isoform. Both proteins were synthesized *in vitro* in rabbit reticulocyte lysate (RRL) in the ratio of approximately 1:1 when the uncapped p53-FL template was used. With the same but capped template, the ratio increased to 5:1 in favor of the full-length protein showing clearly that translation was cap-dependent in these conditions (Figure 6). More detailed translational studies were performed with the p53-554 RNA, which comprised the 5′ UTR and roughly half of the p53 protein-coding portion and which ended with the UGA stop codon. Three other derivatives of this RNA were also synthesized (Figure 1). A thermodynamically stable hairpin with $\Delta G = -39.4$ kcal/mol[30] was introduced at the 5′ end of Hp53-554 RNA. Hairpin insertions are frequently used as a tool to inhibit ribosome scanning of the mRNA, thereby suppressing cap-dependent translation initiation.[30] The initiation codon AUG1 was mutated to GCG triplet in p53-554(mut) RNA; thus, translation of this template could occur only from the AUG2 codon. Both these changes, the stable hairpin and mutated AUG1, were present in Hp53-554(mut) RNA. The secondary structures of Hp53-554 RNA, p53-554(mut) RNA, and Hp53-554(mut) RNA were analyzed using the SHAPE approach, and the results confirmed that the overall folding that was determined for the parental p53-554 RNA was retained in these molecules (data not shown). The four model RNA templates were translated *in vitro* in RRL. Following separation of translation products on SDS gels, the relative amounts of synthesized fragments of p53 protein, p53fr (initiated at AUG1), and ΔN-p53fr (initiated at AUG2) were determined (Figure 6).

With the capped p53-554 RNA, p53fr and ΔN-p53fr proteins were synthesized with the ratio of ca. 5:1 while with the uncapped template the ratio amounted to approximately 2:1 and the lower translation efficiency from AUG1 (0.7) was accompanied by a 2-fold increase of the product initiated from AUG2. With both the capped and uncapped template the ratio of the translation products was similar to that observed with the full-length p53 mRNA (discussed earlier in the text). Thus, p53-554 RNA seems to properly reflect the properties of the full-length p53 mRNA in these translation conditions. The inclusion of the stable hairpin at the 5′ end of Hp53-554 RNA severely inhibited translation from the AUG1 codon (0.08 for capped and 0.19 for uncapped RNA template). Unexpectedly, translation from AUG2 substantially increased (1.35- and 3.2-fold for capped and uncapped message, respectively). Mutation of the first AUG1 codon to GCG in p53-554(mut) RNA resulted in a 3.6-fold increase of translation from AUG2. Interestingly, when the stable hairpin was introduced at the 5′ end of Hp53-554(mut), RNA synthesis from AUG2 was initiated with the same efficiency as in the case of p53-554 RNA template with two initiation codons.

The p53-554 RNA and Hp53-554 RNA were also translated in RRL in the presence of increasing concentration of cap analogue (m^7GpppG) to inhibit cap-dependent translation. In

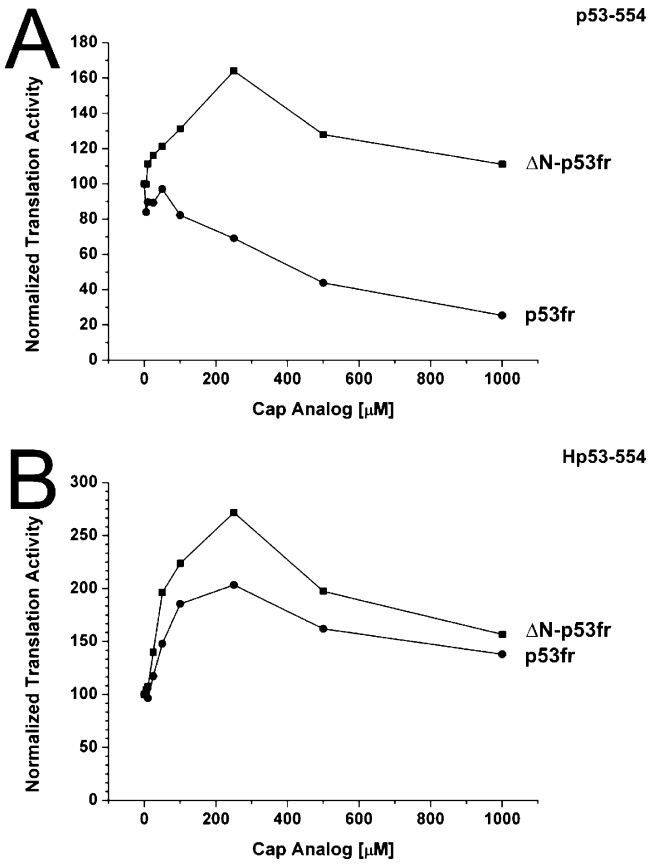

Figure 7. p53-554 RNA (A) and Hp53-554 RNA (B) were translated in RRL in the presence of ^{35}S-methionine and increasing concentration of the cap analogue (m^7GpppG) to inhibit cap-dependent translation. The amounts of p53fr and ΔN-p53fr were determined, and following normalization to the values with no cap analogue added, they were displayed in the figure. The quantitative data presented in panels A and B were calculated based on at least three independent experiments.

the case of p53-554 RNA, translation from AUG1 was inhibited by the cap analogue addition (Figure 7A). The changes were relatively small at low concentration of the inhibitor and did not exceed 30% of the initial value up to 250 μM concentration of the analogue. In contrast, translation from AUG2 showed a remarkable tendency to increase, and at the 250 μM concentration of the cap analogue, translation activity exceeded 160% of the reaction control. An extremely strong effect was observed in translation of Hp53-554 RNA. Translation from both AUG1 and AUG2 codons was increased in a similar manner, reaching ca. 180−200% and 220−270% of the initial values in the presence of cap analogue at a concentration in the range of 100−250 μM (Figure 7B).

Relevance of the Results of This Study to Possible Modes of p53 and ΔN-p53 Translation Initiation. We were curious to know how the results of our *in vitro* translation studies corresponded to the possible modes of initiation of translation of p53 and its N-truncated isoform ΔN-p53. In the scanning model for translation initiation in eukaryotes it has been proposed that the translation efficiency is enhanced when the AUG codon is in the "Kozak's consensus context" of GCCGCC(A/G)CCAUGG.[31] The AUG1 codon is embedded in the sequence ACUGCCAUGGAG, thus adhering well to the Kozak rules. It is assumed that a low level of p53 in the cell is a consequence of its ubiquitination by Mdm2 and subsequent directing to the degradosome.[1−3] However, low efficiency of p53 translation is also observed *in vitro*.[9,32] Interestingly, in the case of the mRNA constructs in which a reporter gene immediately follows the p53 5′ UTR, the amount of synthesized protein substantially increases (ref 7 and unpublished data of our laboratory). This suggests that engagement of the region of mRNA which includes the initiation codon in strong higher order interactions might contribute to the relatively low efficiency of translation initiation, and in consequence, to the low level of p53 protein in the cell. Indeed, already classic studies of Kozak have shown that translation efficiency can be inhibited by highly stable hairpin structures present within the 5′ UTR of mRNAs.[33] More recent studies[30] have investigated the effects of hairpin distance, thermal stability, and GC content on mRNA translation in live mammalian cells and RRL. The results suggest that hairpins with the predicted thermal stabilities stronger than −50 kcal/mol may still be efficiently translated as long as stem GC content is relatively low.[30] Our data showed that the large hairpin domain, which spans nucleotides G56 and C169, and in which the AUG1 codon is located, is relatively stable (ΔG = −52.9 kcal/mol), and its GC content equals 64%. Thus, combination of these two parameters seems to be sufficient to impair but not to block translation initiation.

The N-truncated p53 isoform, ΔN-p53, lacks the first 39 amino acids and originates from alternative translation initiation at an internal AUG codon present within the p53 open reading frame.[4,5] Translation of proteins with alternative initiation codons can occur by reinitiation, by leaky scanning of the ribosome or by an IRES.[31,34,35] As regards ΔN-p53, it is still not known how the isoform is generated in the cell. It has been suggested that it is synthesized by reinitiation from an incompletely spliced mRNA template (p53EII mRNA in which intron 2 has been retained).[36] This proposition is, however, not supported by the observation that p53EII mRNA is much less abundant than the wild-type p53 mRNA in various human cells.[36,37] Moreover, ΔN-p53 is expressed from the wild-type p53 mRNA,[4,5,13] and for instance, in *in vitro* conditions p53 and ΔN-p53 are synthesized at the ratio of approximately 5:1 (Figure 6). The leaky scanning mechanism for p53 mRNA is also not fully compatible with the current thoughts on this alternative way of translation initiation. It is believed that an unfavorable Kozak context allows some ribosomes to bypass the first AUG and thus reach a start codon further downstream.[31,38] In the case of translation of both p53 isoforms the initiation codons are in a similar Kozak context, ACUGCCAUGGAG for the full-length p53 and CAAG-CAAUGGAU for the N-truncated p53 isoform, and both contexts have the −3R/+4G combination. Thus, the primary sequence environment does not follow the simple rule of leaky scanning mechanism, unless we assume that the Kozak rules for the AUG sequence context are substantially modulated by the involvement of this region in higher-order RNA structure.

Finally, it is interesting whether our results are relevant to the recent proposition that translation of p53 and its ΔN-p53 isoform may be initiated by internal initiation mechanism with the use of IRES elements.[7,16] In the reported studies mRNA constructs have been used in which the 5′ untranslated regions of p53 mRNA were directly attached to the sequences encoding reporter proteins. Yang et al.[7] have exclusively investigated a p53 5′ UTR version consisting of 131 nucleotides, whereas

Ray et al.[16] have also analyzed the functional properties of the 251 nucleotides long 5′ untranslated sequence which is responsible for translation initiation of ΔN-p53. We showed that the secondary structure fold of the p53 5′ UTR involved a part of the downstream p53 coding sequence and that this structure is preserved in the full-length mRNA. The only secondary structure motif common to both short and long 5′ noncoding regions, which could be important for their ability to act as IRES elements, is a small hairpin G106-C120 (Figures 2 and 3). Interestingly, although Ray et al.[16] have postulated two different IRES elements to exist, they do not exclude the possibility that only one IRES is present in the p53 mRNA, which alternatively allows translation initiation from two different downstream initiation codons. An IRES element has been also suggested by Candeias et al.[37] to direct translation of both the p53 protein isoforms. On the basis of the results of several elegant experiments, the authors proposed that the sequence encoding the first 40 amino acids of p53 harbors the IRES. They observed that inhibition of cap-dependent translation from AUG1 paves the way for cap-independent initiation from AUG2, promoting the synthesis of ΔN-p53.[37] It has to be noted, however, that the majority of their model mRNA constructs were deprived of the 5′ UTR; thus, the functional role of this region remained largely undefined.[37,39]

Our results of translation of p53-554 RNA in RRL confirmed that translation initiation from AUG1 was mostly cap-dependent in these conditions (Figures 6 and 7). As expected, the process was stimulated by the presence of the cap structure and was strongly inhibited (to 1/10 of its initial value) by a stable hairpin present at the 5′ end of the Hp53-554 RNA template. One may speculate that the remaining protein fraction was synthesized in a cap-independent process. Strong stimulation of translation of Hp53-554 RNA from AUG1 by the cap analogue suggests the presence of an IRES.[40,41] It has earlier been proposed that the increase in the translation of an mRNA in the presence of cap analogue implies the possibility of competition between the cap structure and the IRES for the translational machinery.[42]

The translation initiation from AUG2 showed a largely cap-independent character. Addition of the cap structure at the 5′ end of p53-554 RNA and Hp53-554 RNA templates did not stimulate (but actually decreased) initiation from this site. This argues against a leaky scanning mechanism but might be interpreted as the presence of an IRES.[40] Moreover, blocking cap-dependent translation from AUG1 by the stable hairpin at the template 5′ end did not change the level of initiation from AUG2, and upon addition of the cap analogue, translation from AUG2 increased even strongly, which again suggests the presence of an IRES.[40,41]

Our observations were generally consistent with those described by Candeias et al.[37] on translation initiation of the p53 mRNA. However, in several experiments they have used model RNA templates which have been deprived of the p53 5′ UTR. It might explain some results different from those that we found in our study. Specifically, in the presence of increasing concentration of the cap analogue the authors observed strong reduction of translation efficiency from AUG1 and almost no change from AUG2.[37] In a similar experiment with p53-554 RNA with the 5′ UTR we observed a relatively slow decrease in translation from AUG1 and strong increase from AUG2. Upon inhibition of cap-dependent translation by the hairpin structure in Hp53-554 RNA the remaining translation from AUG1 was strongly stimulated by the cap analogue (Figure 7B). These differences pointed out to a substantial role of the 5′ UTR in p53 translation.

DISCUSSION

We compared the secondary structure folding of two p53 mRNA fragments: p53utr RNA, corresponding to the 5′ UTR for the full-length p53 protein, and ΔN-p53utr RNA, containing an additional stretch of the coding sequence with the initiation codon for the ΔN-p53 isoform (Figure 1). It turned out that the secondary structure of the isolated 5′ UTR did not reflect the structure of this region in the context of a longer mRNA fragment. A part of the p53 coding sequence was involved in the folding of the corresponding region in ΔN-p53utr RNA (Figures 2 and 3). This characteristic secondary structure was also found in the 5′-terminal region of the p53-554 RNA consisting of the 5′ UTR and roughly half of the p53 coding sequence. Also, in the full-length p53 mRNA, which included 5′ UTR, a coding sequence, and 3′ UTR, the 5′-terminal region was arranged in a highly similar manner (Figure 4 and Figures S3−S5). Recently, it has been suggested that in the binding of ribosomal protein L26 and p53 translational stimulation a double-stranded RNA region containing complementary sequences of the 5′ and 3′ UTRs is involved.[11] However, our results of structural mapping of these regions in the full-length p53 mRNA and in its 5′-terminal fragments did not show direct 5′ UTR−3′ UTR interactions in the applied conditions.

Our observation that the p53utr RNA does not preserve its secondary structure when extended in the 3′ direction, as in ΔN-p53utr RNA, has some important implications. It has been suggested that functioning of 5′ untranslated regions of several mRNAs in the regulation of translation depends on the folding of these regions in higher order structures.[43−45] Such RNA structures may attract specific proteins or act as IRES elements. In particular, the 5′ untranslated region of p53 mRNA is able to bind several proteins—p53,[8,9] PTB,[12] nucleolin, and ribosomal protein L26[9,11]—and this region seems to direct the cap-independent translation process.[7,16] However, in several earlier studies, the p53 5′ untranslated sequence has been directly attached to a sequence encoding a reporter protein. Our data suggest that in such message constructs the secondary structure of the 5′ noncoding region might differ substantially from that of the full-length p53 mRNA.

The most characteristic structural elements in the 5′-terminal region of p53 mRNA were two hairpin motifs. In the first hairpin, the initiation AUG1 codon was embedded (Figure 4), while the other hairpin has been earlier shown to bind to the Mdm2 protein.[13,14] Moreover, localization of both the initiation triplets AUG1 and AUG2 at the helix−bulge junctions suggested that their use might be regulated through induction of RNA structural changes in their vicinity (Figures 4 and 5). Indeed, thermal melting studies showed that the structural environment of the AUG1 codon as well as the elements possibly involved in the binding of Mdm2 and PTB melted at lower temperatures than other parts of the RNA structure (Figure S8). A similar situation of base pairing interactions between nucleotides within the AUG codon has been observed in the yeast URE2 mRNA, and the authors suggest that unwinding this structure is an important step in the internal translation initiation.[46] The structural environment which embeds the AUG start codons in a structural context neither

freely accessible in single-stranded stretches nor highly constrained in rigid helices may be crucial for the regulation of translation initiation.

Alternative mechanisms of p53 mRNA translation initiation that control expression of the full-length p53 protein and ΔNp53 isoform were also investigated *in vitro* in the rabbit reticulocyte lysate system. The p53-554 RNA template was used in detailed studies. Derivatives of this template had an additional, thermodynamically stable hairpin at the 5′ end or the initiation AUG1 codon mutated to GCG triplet. The model RNA templates were also translated in the presence of a cap analogue to inhibit cap-dependent translation (Figures 6 and 7). The results confirmed that translation initiation from AUG1 was mostly cap-dependent. As expected, the process was stimulated by the presence of a cap structure and strongly inhibited by the hairpin at the template 5′ end. One might speculate that upon inhibition the remaining protein fraction was synthesized in a cap-independent process. Strong stimulation of its synthesis by the cap analogue suggested the presence of an IRES.[40,41] The translation initiation from AUG2 showed a largely cap-independent character. Addition of the cap structure at the 5′ end of RNA templates did not stimulate (but actually decreased) initiation from this site. This argues against a leaky scanning mechanism but might be interpreted as the presence of an IRES.[40] Moreover, blocking cap-dependent translation from AUG1 by the stable hairpin did not change the level of initiation from AUG2. Upon addition of the cap analogue, translation from AUG2 increased even stronger, which again suggested the presence of an IRES.[40,41]

The 5′ terminal sequence of p53 is conserved in many mammalian species including human, chimpanzee, rhesus, pig, rabbit, sheep, cat, guinea pig, cow, mouse, and rat (Figure S9). A puzzling observation is that in some sequences the initiation codon for the ΔN-p53 isoform does not seem to be present in the expected position. It has earlier been reported to be present in p53 gene of cow, *Xenopus*, rhesus, horse, and pig,[4] and we showed that it also occurred in the genes of rabbit and sheep (Figure S9). Consequently, it has been suggested that expression of ΔN-p53 isoform may be restricted to some species.[4] We noticed, however, that in rhesus an AUG codon is located four triplets downstream, similarly, as it is in humans. In the corresponding position, or triplet positions immediately adjacent, CUG codons exist in the sequences of pig, rabbit, sheep, and cow (data not shown). Interestingly, CUG and ACG are most efficiently recognized as non-AUG initiation codons in RRL.[47] Although so far only a few examples of translation initiation at non-AUG triplets have been reported, such a possibility might be worth testing experimentally for the N-truncated p53 isoform.

Finally, it has to be taken into consideration that the structure and functional properties of the 5′-terminal region of p53 mRNA might be modulated in the cell by interactions with several proteins, in particular those playing the role of ITAF factors. The function of one of such factors, the polypyrimidine tract-binding protein (PTB), which seems to specifically interact with the 5′-terminal region of p53 mRNA,[12] is currently being evaluated in our laboratory.

■ ASSOCIATED CONTENT

Ⓢ Supporting Information

Autoradiograms of SHAPE analysis of ΔN-p53utr, p53utr, p53-554, H56-169, and p53-FL RNAs (Figures S1−S3); autoradiograms of Pb^{2+}-induced cleavage analysis of p53-554 and p53-FL RNAs (Figures S4 and S5); nuclease mapping data for p53-FL and ΔN-p53utr RNAs (Figure S6); structural probing data for H56-169 (Figure S7); temperature melting data of ΔN-p53utr RNA followed by SHAPE (Figure S8); multiple alignment of 5′-terminal regions of p53 mRNA in mammals (Figure S9). This material is available free of charge via the Internet at http://pubs.acs.org.

■ AUTHOR INFORMATION

Corresponding Author

*Tel: +48 61 8528503; Fax: +48 61 8520532; e-mail: ciesiolk@ibch.poznan.pl.

Funding

This work was supported by the Polish Ministry of Science and Higher Education (grant NN301272037 to J.C.).

■ ACKNOWLEDGMENTS

We thank members of our laboratory for valuable comments on the manuscript. Drs Michal Legiewicz and Katarzyna Purzycka are thanked for helpful suggestions on SHAPE protocols and data analysis.

■ ABBREVIATIONS

IRES, internal ribosome entry site; ORF, open reading frame; UTR, untranslated region; RRL, rabbit reticulocyte lysate; RT, reverse transcription; SHAPE, selective 2′-hydroxyl acylation analyzed by primer extension; NMIA, *N*-methylisatoic anhydride.

■ REFERENCES

(1) Mills, A. A. (2005) p53: link to the past, bridge to the future. *Genes Dev. 19*, 2091−2099.

(2) Römer, L., Klein, C., Dehner, A., Kessler, H., and Buchner, J. (2006) p53 - a natural cancer killer: structural insights and therapeutic concepts. *Angew. Chem., Int. Ed. 45*, 6440−6460.

(3) Olivier, M., Petitjean, A., Marcel, V., Pétré, A., Mounawar, M., Plymoth, A., de Fromentel, C. C., and Hainaut, P. (2009) Recent advances in p53 research: an interdisciplinary perspective. *Cancer Gene Ther. 16*, 1−12.

(4) Courtois, S., Verhaegh, G., North, S., Luciani, M. G., Lassus, P., Hibner, U., Oren, M., and Hainaut, P. (2002) ΔN-p53, a natural isoform of p53 lacking the first transactivation domain, counteracts growth suppression by wild-type p53. *Oncogene 21*, 6722−6728.

(5) Yin, Y., Stephen, C. W., Luciani, M. G., and Fåhraeus, R. (2002) p53 stability and activity is regulated by Mdm2-mediated induction of alternative p53 translation products. *Nat. Cell Biol. 4*, 462−467.

(6) Grover, R., Candeias, M. M., Fåhraeus, R., and Das, S. (2009) p53 and little brother p53/47: linking IRES activities with protein functions. *Oncogene 28*, 2766−2772.

(7) Yang, D. Q., Halaby, M. J., and Zhang, Y. (2006) The identification of an internal ribosomal entry site in the 5′-untranslated region of p53 mRNA provides a novel mechanism for the regulation of its translation following DNA damage. *Oncogene 25*, 4613−4619.

(8) Mosner, J., Mummenbrauer, T., Bauer, C., Sczakiel, G., Grosse, F., and Deppert, W. (1995) Negative feedback regulation of wild-type p53 biosynthesis. *EMBO J. 14*, 4442−4449.

(9) Takagi, M., Absalon, M. J., McLure, K. G., and Kastan, M. B. (2005) Regulation of p53 translation and induction after DNA damage by ribosomal protein L26 and nucleolin. *Cell 123*, 49−63.

(10) Riley, K. J.-L., and Maher, L. J. III (2007) p53-RNA interactions: new clues in an old mystery. *RNA 13*, 1825−1833.

(11) Chen, J., and Kastan, M. B. (2010) 5′-3′-UTR interactions regulate p53 mRNA translation and provide a target for modulating p53 induction after DNA damage. *Genes Dev. 24*, 2146−2156.

(12) Grover, R., Ray, P. S., and Das, S. (2008) Polypyrimidine tract binding protein regulates IRES-mediated translation of p53 isoforms. *Cell Cycle 7*, 2189−2198.

(13) Candeias, M. M., Malbert-Colas, L., Powell, D. J., Daskalogianni, C., Maslon, M. M., Naski, N., Bourougaa, K., Calvo, F., and Fåhraeus, R. (2008) p53 mRNA controls p53 activity by managing Mdm2 functions. *Nat. Cell Biol. 10*, 1098−1105.

(14) Naski, N., Gajjar, M., Bourougaa, K., Malbert-Colas, L., Fåhraeus, R., and Candeias, M. M. (2009) The p53 mRNA-Mdm2 interaction. *Cell Cycle 8*, 31−34.

(15) Mahmoudi, S., Henriksson, S., Corcoran, M., Méndez-Vidal, C., Wiman, K. G., and Farnebo, M. (2009) Wrap53, a natural p53 antisense transcript required for p53 induction upon DNA damage. *Mol. Cell 33*, 462−471.

(16) Ray, P. S., Grover, R., and Das, S. (2006) Two internal ribosome entry sites mediate the translation of p53 isoforms. *EMBO Rep. 7*, 404−410.

(17) Das, R., Laederach, A., Pearlman, S. M., Herschlag, D., and Altman, R. B. (2005) SAFA: Semi-automated footprinting analysis software for high-throughput quantification of nucleic acid footprinting experiments. *RNA 11*, 344−354.

(18) Vicens, Q., Gooding, A. R., Laederach, A., and Cech, T. R. (2007) Local RNA structural changes induced by crystallization are revealed by SHAPE. *RNA 13*, 536−548.

(19) Mathews, D. H., Disney, M. D., Childs, J. L., Schroeder, S. J., Zuker, M., and Turner, D. H. (2004) Incorporating chemical modification constraints into a dynamic programming algorithm for prediction of RNA secondary structure. *Proc. Natl. Acad. Sci. U. S. A. 101*, 7287−7292.

(20) Wilkinson, K. A., Gorelick, R. J., Vasa, S. M., Guex, N., Rein, A., Mathews, D. H., Giddings, M. C., and Weeks, K. M. (2008) High-throughput SHAPE analysis reveals structures in HIV-1 genomic RNA strongly conserved across distinct biological states. *PLoS Biol. 6*, e96.

(21) Tuck, S. P., and Crawford, L. (1989) Characterization of the human p53 gene promoter. *Mol. Cell. Biol. 9*, 2163−2172.

(22) Ciesiołka, J., Michałowski, D., Wrzesinski, J., Krajewski, J., and Krzyżosiak, W. J. (1998) Patterns of cleavages induced by lead ions in defined RNA secondary structure motifs. *J. Mol. Biol. 275*, 211−220.

(23) Kirsebom, L. A., and Ciesiołka, J. (2005) Pb^{2+}-induced cleavage of RNA, in *Handbook of RNA Biochemistry*, pp 214−228, Wiley-VCH Verlag GmbH & Co. KGaA, Weinheim.

(24) Huntzinger, E., Possedko, M., Winter, F., Moine, H., Ehresmann, C., and Romby, P. (2005) Probing RNA structures with enzymes and chemicals *in vitro* and *in vivo*, in *Handbook of RNA Biochemistry*, pp 151−171, Wiley-VCH Verlag GmbH & Co. KGaA, Weinheim.

(25) Matysiak, M., Wrzesiński, J., and Ciesiołka, J. (1999) Sequential folding of the genomic ribozyme of the hepatitis delta virus: structural analysis of RNA transcription intermediates. *J. Mol. Biol. 291*, 283−294.

(26) Dutkiewicz, M., and Ciesiołka, J. (2005) Structural characterization of the highly conserved 98-base sequence at the 3′ end of HCV RNA genome and the complementary sequence located at the 5′ end of the replicative viral strand. *Nucleic Acids Res. 33*, 693−703.

(27) Dutkiewicz, M., Świątkowska, A., Figlerowicz, M., and Ciesiołka, J. (2008) Structural domains of the 3′-terminal sequence of the hepatitis C virus replicative strand. *Biochemistry 47*, 12197−12207.

(28) Wilkinson, K. A., Merino, E. J., and Weeks, K. M. (2006) Selective 2′-hydroxyl acylation analyzed by primer extension (SHAPE): quantitative RNA structure analysis at single nucleotide resolution. *Nature Protoc. 1*, 1610−1616.

(29) Wilkinson, K. A., Vasa, S. M., Deigan, K. E., Mortimer, S. A., Giddings, M. C., and Weeks, K. M. (2009) Influence of nucleotide identity on ribose 2′-hydroxyl reactivity in RNA. *RNA 15*, 1314−1321.

(30) Babendure, J. R., Babendure, J. L., Ding, J. H., and Tsien, R. Y. (2006) Control of mammalian translation by mRNA structure near caps. *RNA 12*, 851−861.

(31) Kozak, M. (2005) Regulation of translation *via* mRNA structure in prokaryotes and eukaryotes. *Gene 361*, 13−37.

(32) Ofir-Rosenfeld, Y., Boggs, K., Michael, D., Kastan, M. B., and Oren, M. (2008) Mdm2 regulates p53 mRNA translation through inhibitory interactions with ribosomal protein L26. *Mol. Cell 32*, 180−189.

(33) Kozak, M. (1989) Circumstances and mechanisms of inhibition of translation by secondary structure in eukaryotic mRNAs. *Mol. Cell. Biol. 9*, 5134−5142.

(34) Kochetov, A. V., Ahmad, S., Ivanisenko, V., Volkova, O. A., Kolchanov, N. A., and Sarai, A. (2008) uORFs, reinitiation and alternative translation start sites in human mRNAs. *FEBS Lett. 582*, 1293−1297.

(35) Kochetov, A. V. (2008) Alternative translation start sites and hidden coding potential of eukaryotic mRNAs. *Bioessays 30*, 683−691.

(36) Ghosh, A., Stewart, D., and Matlashewski, G. (2004) Regulation of human p53 activity and cell localization by alternative splicing. *Mol. Cell. Biol. 24*, 7987−7997.

(37) Candeias, M. M., Powell, D. J., Roubalova, E., Apcher, S., Bourougaa, K., Vojtesek, B., Bruzzoni-Giovanelli, H., and Fåhraeus, R. (2006) Expression of p53 and p53/47 are controlled by alternative mechanisms of messenger RNA translation initiation. *Oncogene 25*, 6936−6947.

(38) Smith, E., Meyerrose, T. E., Kohler, T., Namdar-Attar, M., Bab, N., Lahat, O., Noh, T., Li, J., Karaman, M. W., Hacia, J. G., et al. (2005) Leaky ribosomal scanning in mammalian genomes: significance of histone H4 alternative translation *in vivo*. *Nucleic Acids Res. 4*, 1298−1308.

(39) Bourougaa, K., Naski, N., Boularan, C., Mlynarczyk, C., Candeias, M. M., Marullo, S., and Fåhraeus, R. (2010) Endoplasmic reticulum stress induces G2 cell-cycle arrest via mRNA translation of the p53 isoform p53/47. *Mol. Cell 38*, 78−88.

(40) Beaudoin, M. E., Poirel, V. J., and Krushel, L. A. (2008) Regulating amyloid precursor protein synthesis through an internal ribosomal entry site. *Nucleic Acids Res. 36*, 6835−6847.

(41) Vallejos, M., Ramdohr, P., Valiente-Echeverría, F., Tapia, K., Rodriguez, F. E., Lowy, F., Huidobro-Toro, J. P., Dangerfield, J. A., and López-Lastra, M. (2010) The 5′-untranslated region of the mouse mammary tumor virus mRNA exhibits cap-independent translation initiation. *Nucleic Acids Res. 38*, 618−632.

(42) Dobson, T., Minic, A., Nielsen, K., Amiott, E., and Krushel, L. (2005) Internal initiation of translation of the TrkB mRNA is mediated by multiple regions within the 5′ leader. *Nucleic Acids Res. 33*, 2929−2941.

(43) Halaby, M. J., and Yang, D. Q. (2007) p53 translational control: a new facet of p53 regulation and its implication for tumorigenesis and cancer therapeutics. *Gene 395*, 1−7.

(44) Sonenberg, N., and Hinnebusch, A. G. (2009) Regulation of translation initiation in eukaryotes: mechanisms and biological targets. *Cell 136*, 731−745.

(45) Van Der Kelen, K., Beyaert, R., Inzé, D., and De Veylder, L. (2009) Translational control of eukaryotic gene expression. *Crit. Rev. Biochem. Mol. Biol. 44*, 143−168.

(46) Reineke, L. C., Komar, A. A., Caprara, M. G., and Merrick, W. C. (2008) A small stem-loop element directs internal initiation of the URE2 internal ribosome entry site in *Saccharomyces cerevisiae*. *J. Biol. Chem. 283*, 19011−19025.

(47) Peabody, D. S. (1989) Translation initiation at non-AUG triplets in mammalian cells. *J. Biol. Chem. 264*, 5031−5035.